



COVER SHEET

This is the author-version of article published as:

Frost, Ray and Reddy, Lakshmi and Reddy, Gangi and Reddy, Siva and Reddy, Jagannatha (2006) Characterization of clinohumite by selected spectroscopic methods. *Spectrochimica Acta* 65(3-4):pp. 684-688.

Copyright 2006 Elsevier

Accessed from <http://eprints.qut.edu.au>

CHARACTERIZATION OF CLINOHUMITE BY SELECTED SPECTROSCOPIC METHODS

S. Lakshmi Reddy ¹, N.C. Gangi Reddy ², G. Siva Reddy ², B. Jagannatha Reddy ³
and Ray L Frost ^{3*}

1. Dept. of Physics, S.V.D.College, Kadapa 516 003, India.

2. Dept. of Chemistry, S.V.U.P.G.Centre, Kadapa 516 003, India

3. Inorganic Materials Research Program, Queensland University of Technology, 2
George Street, Brisbane, GPO Box 2434, Queensland 4001, Australia

Abstract

Clinohumite, a humite group mineral, originated from Pamir Mountains, USSR is used in the present work. Optical absorption, electron paramagnetic resonance (EPR), near infrared (NIR) and Mossbauer techniques are used in the characterization of the mineral sample. The optical absorption spectrum indicates that Fe(II) impurity is present in two sites with distorted octahedral structure. NIR results are attributed to water fundamentals. EPR studies on powder sample confirm the presence of Mn(II) in three different sites and also an iron impurity. Mossbauer studies confirm the presence of iron impurity in two different sites.

* Author to whom correspondence should be addressed (r.frost@qut.edu.au)
P: +61 7 3864 2407 F: +61 7 3864 1804

Keywords: humite, clinohumite, electron paramagnetic resonance, near infrared spectroscopy, Mossbauer spectroscopy, optical absorption, electron paramagnetic resonance

1. Introduction

Manganese is the 10th most abundant element in the Earth's crust and second only to iron as the most common heavy metal. Crustal rocks contain usually 0.1 % Mn [1]. Most of the silicates; oxide and or hydroxide minerals contain mainly the two transition metals, Fe and Mn [2]. Clinohumite is a silicate mineral belonging to humite group (also known as chondrodite group). The humite series of minerals have the general formula $n[\text{Mg}_2\text{SiO}_4] [\text{Mg}(\text{OH},\text{F})_2]$. This group of minerals is classified as follows [3]:

Norbergite	$\text{Mg}_3(\text{SiO}_4)(\text{F},\text{OH})_2$
Chondrodite	$(\text{Mg},\text{Fe}^{2+})_5(\text{SiO}_4)_2(\text{F},\text{OH})_2$
Humite	$(\text{Mg},\text{Fe}^{2+})_7(\text{SiO}_4)_3(\text{F},\text{OH})_2$
Clinohumite	$(\text{Mg},\text{Fe}^{2+})_9(\text{SiO}_4)_4(\text{F},\text{OH})_2$

In the above group of minerals, Mg(II) can be replaced by divalent calcium, iron, titanium, manganese and zinc. The crystal structure of the clinohumite is similar to other members of the humite group of minerals. It is noted for having a mixture of silicate layers and oxide layers in its structure [4-7]. The parameters of the monoclinic cell, with space group $P2_1/b$ are $a = 0.4744$, $b = 1.0250$, $c = 1.3664$ nm, and $\alpha = 100.786^\circ$. The structure is based on a slightly distorted hexagonal close-packed array of anions and are similar to those of other humite minerals and to the olivines. There are five distinct

octahedral sites in clinohumite. Of these, $M(1)_c$ and $M(2)_6$ are like those in the olivines and $M(1)_N$, $M(2)_5$, $M(3)$ are those in humite. One-half the octahedral sites and one-ninth the tetrahedral sites are filled. The distribution of transition metal ions in clinohumite is consistent with that in humite and chondrodite, Fe(II) being in more distorted MO_6 structure [6]. The chemical analysis of this group of minerals indicates that substitution of Mg by iron, Mn and Ti ranges from 0.4 to 7.3, 0 to 1.05 and 0 to 3.24 wt % respectively [8].

Detailed spectral studies have been reported on humite but not on clinohumite [9]. The study of clinohumite, originating from Pamir Mountains, USSR is undertaken in the present work. Optical absorption and Mossbauer spectral studies of clinohumite mineral originating from Kugda and Khilan, USSR show the presence of iron and titanium in this mineral [10]. The authors present here a detailed study on clinohumite by EPR, optical absorption and Mössbauer spectroscopic techniques.

2. Experimental

A light yellow colored clinohumite $(Mg,Fe^{2+})_9(SiO_4)_4(F,OH)_2$ sample was supplied by Ward's, New York, USA. A finely powdered sample of the mineral is taken in a quartz tube (free from iron and manganese impurities) for EPR measurements. The spectra of the powdered sample are recorded at room (RT) and liquid nitrogen temperatures (77 K) on JEOL JES-TE100 ESR spectrometer operating at X-band frequencies ($\nu = 9.40584$ GHz), having a 100 KHz field modulation to obtain the first derivative EPR spectrum. DPPH with a g value of 2.0036 is used for g factor calculations. Optical absorption spectrum of the compound is recorded at RT on Carey

5E UV Vis-NIR spectrophotometer in mull form in the range 200-2000 nm. Mössbauer measurements were performed with a conventional constant-acceleration Spectrometer in transmission geometry with a source of 50 mCi ^{57}Co in a Rh matrix. All isomer shifts are given relative to that of $\alpha\text{-Fe}$ at room temperature.

3. Results and discussion

The ground state configuration of Fe(II) ion is $3d^6$. The configuration can be expressed as $t_{2g}^4 e_g^2$ for high spin octahedral field. Hence, the energy states are $^5T_{2g}$, 3E_g , $^3T_{2g}$ and some more triplets and singlets of which $^5T_{2g}$ forms the ground state. The other excited configurations, such as $t_{2g}^3 e_g^3$ gives rise to a several triplet and singlet states and one quintet state designated as 5E_g . Thus the spin allowed transition $^5T_{2g} \rightarrow ^5E_g$ is expected to be strong and all other spin forbidden transitions are very weak [11, 12]. So, the $^5T_{2g} \rightarrow ^5E_g$ transition gives an intense, but broad absorption band. Often this band splits into two in an octahedral environment. The splitting of this band may be explained in terms of one or more of the following: (i) spin orbit coupling, (ii) static distortion of the octahedron and (iii) dynamic Jahn-Teller effect [13]. If the splitting is due to spin-orbit coupling, the splitting value is about 100 cm^{-1} . On the other hand, if the splitting is of the order of 2000 cm^{-1} , then it is due to static distortion of octahedron [13-15]. An intermediate value between 100 and 2000 cm^{-1} indicates a dynamic Jahn-Teller effect in the excited 5E_g state [16-17]. In the latter case, the energy level split symmetrically to the center of gravity and the average of these values of these bands is to be taken as $10Dq$ value.

3.1. Mössbauer studies

The Mössbauer spectrum of clinohumite recorded at 296 K fits well with characteristic pattern of the Zeeman hyperfine splitting of iron sample shown in Fig.1. The spectrum shows the magnetic ordering of the sample. The sample does not exhibit any net magnetization ($B = 0$ Tesla) and hence it is not ferromagnetic. From the spectrum, the Mossbauer constants quadrupole splitting (QS), isomer shift (IS), line width (Γ) and percentage of area (I%) are calculated and given in Table 1 along with the values reported for similar systems. These values indicate that iron in the sample is in Fe(II) and Fe(III) states. Since the ligands are bound to iron in two different ways and they give different amounts of charge density around metal ion. The Mössbauer data suggest the presence of 72% Fe(II) in D site and 27% Fe(III) in the L site. Further a comparison of these values is also made with the Mössbauer parameters of other iron containing systems of known crystal structures [18-22, 24] and is in good agreement with the present data.

3.2 Optical absorption spectrum

Optical absorption spectrum of clinohumite, recorded at room temperature in the range 200 to 2000 nm in mull form, is shown in Fig. 2 (a). It consists of bands at 23800, 23260, 16670, 15625, 10360, 9800, 9130, 8300, 7435, 7290, 6870, 5900, 5850, 5690 and 5480 cm^{-1} . For easy analysis of the spectrum, the bands are divided into two sets as 9130, 10360, 15625, 23260 cm^{-1} and 8300, 9800, 16670, 23800 cm^{-1} .

The two bands observed in the first set at 10360 and 9130 cm^{-1} are broad and intense and 9800, along with 8300 cm^{-1} in the second set, are assigned to the two components of the same transition ${}^5T_{2g} \rightarrow {}^5E_g$ and the average of these bands, i.e., 9745 cm^{-1} and 9050 cm^{-1} is taken as $10Dq$. Accordingly the Dq value is different for both sites as 975 and 905 cm^{-1} . The splitting of $10Dq$ band ($10360 - 9130 = 1230 \text{ cm}^{-1}$ and $9800 - 8300 =$

1500 cm⁻¹ indicates that it is due to dynamic Jahn-Teller effect in the excited ⁵E_g state since the splitting value is an intermediate between 100 and 2000 cm⁻¹. The Tanabe-Sugano diagram of d⁶ configuration is used to assign the transitions of the other bands [25]. The energy matrices of d⁶ configuration are solved for different values of Racah parameters Dq, B and C for both sites. The parameters that give good fit to the experimental data for site one are Dq = 975 cm⁻¹, B = 900 cm⁻¹ and C = 4700 cm⁻¹ and for site two are Dq = 905 cm⁻¹, B = 850 cm⁻¹ and C = 4800 cm⁻¹. The data and their assignments along with the calculated values are presented in Table 2 for both sites of Fe(II) in the mineral. As a comparison, the crystal field parameters for other samples are given in Table 2. For free ferrous ion B¹ = 1060 cm⁻¹. The percentage ratio of observed B value to free ferrous ion B¹ value is defined as nephelauxetic ratio ($\beta = \frac{B}{B^1}$). It is also calculated and its value is given in Table 3, along with the values reported for similar systems. These are in good agreement with the present work. The above data suggest that Fe(II) ion occupies different sites in the mineral.

3.3. EPR results

A typical EPR spectrum of the sample recorded at room temperature is given in Fig. 3. It is well known that in the transition metal ion EPR studies, Mn(II) is easily observable at room temperature, even if present in minute levels, compared to other ions, including Cu(II) impurity. Fig. 3 clearly indicates the presence of Mn(II) in the sample. An expanded version of central sextet is shown (frequency =9.40584 GHz. Power = 1.0 mW, modulation field 0.2 mT) in Fig. 4. Mn(II), being a d⁵ ion, has total spin S = 5/2. This state splits into three Kramers' doublets, $\pm 5/2$ >, $\pm 3/2$ > and $\pm 1/2$ > separated by 4D and 2D respectively. Here, D is the zero-field splitting parameter. These three doublets split

into six energy levels by the application of an external magnetic field. Transitions between these six energy levels will give rise to five resonance lines. Each of these resonance lines splits into a sextet, due to the interaction of the electron spin with the nuclear spin of ^{55}Mn , which is $5/2$. Thus, one expects a 30 line pattern. However, depending on the relative magnitudes of D and A (hyperfine coupling constant of manganese), these 30 lines will appear as a separate bunch of 30 lines or 6 lines (if $D = 0$). The separation between the extreme set of resonance lines is approximately equal to $8D$ (first order). However, in a few cases, deviation from axial symmetry leads to a term, known as E, in the spin Hamiltonian. The value of E can be easily calculated from single crystal measurements. A non-zero value for E results in making the spectrum unsymmetrical about the central sextet. Fig. 3 contains a strong sextet at the centre of the spectrum corresponding to the electron spin transition $+1/2 \rightarrow -1/2$. Generally, in most cases, the powder spectrum is characterized by a sextet, corresponding to this transition. The other four transitions, corresponding to $\pm 5/2 \leftrightarrow \pm 3/2$ and $\pm 3/2 \leftrightarrow \pm 1/2$ are not seen due to their high anisotropy in D. However, a few cases are known in the literature, where all the transitions are seen. Moreover, the low field transitions are more intense than high field transitions. To know the intensity of low field and high field transitions in the spectrum, modulation is changed from 0.2 mT to 1.0 mT in low and high fields with out change in magnetic field scale and the same is recorded on the two sides of the above the Fig.3. Thus, the latter are seen at higher gains of the spectrometer. In addition, if $E \neq 0$, the EPR spectrum will not be symmetrical about the central sextet. The expanded version of the powder spectrum (Fig. 4) indicates the presence of at least three types of Mn(II) impurities in the mineral. The sixth manganese hyperfine resonance clearly contains three lines (marked by a, b and c). The third Mn(II) site is of very low

intensity. The extra set of resonances in between the main sextet is due to the forbidden transitions. From the powder spectrum of the mineral, the following parameters have been calculated:

Site I: $g = 2.000(1)$, $A = 9.15(2)$ mT; and $D = 43.8(1)$ mT.

Site II: $g = 2.003(2)$, $A = 9.23(2)$ mT; and $D = 44.1(1)$ mT.

Site III: $g = 2.007(1)$, $A = 9.40(2)$ mT; and $D = 44.1(1)$ mT.

This large value of D indicates a considerable amount of distortion around the central metal ion. The Mössbauer and optical spectra have been analyzed by considering two types of iron impurities. As EPR is highly sensitive to Mn(II) impurity, three such sites have been determined in the EPR spectrum. These two sites have close spin Hamiltonian parameters. EPR spectrum indicates a non-zero value for E , which is very difficult to estimate from the powder spectrum. Cooling the sample does not change the general nature of the spectrum.

A close look at the centre of the EPR spectrum indicates a broad line underneath the Mn(II) sextet. This can be attributed to the iron impurity in the sample. Generally, Fe(III) and Fe(II) impurities will give rise to a broad line around $g = 2$. Except stating the presence of iron impurity, no extra information can be obtained from the powder spectrum recorded at room temperature and low temperature. Even though the percentage of iron is more than that of manganese, its intensity is relatively smaller compared to the signals obtained from the manganese impurity. This can be explained below.

Generally, whenever a mineral is formed under the earth, the nearby impurities will enter the mineral in various locations such as interstitial, substitutional or both.

However, due to thermal conditions present during mineral growth, all the impurities will not be present at the lowest minimum energy configurations. From our previous studies [29, 30], it has been confirmed that heat treatment of the sample has resulted in transferring the impurities, which are in different energy locations to the lowest minimum energy configuration. Hence the sample has been subjected to heat treatment around 620 K for about 4, 8, 12 and 16 hours. The EPR spectrum, recorded at each heat treatment indicates a slow increase in the intensity of the broad line at $g = 2$. However, the general nature of three impurities is same with respect to g , A and D values. This confirms that heat treatment has resulted in transferring the ions at different energy locations on the energy surface to its lowest energy configuration. Due to the very low percentage of TiO_2 , its resonances are not seen. Depending on the charge considerations, the impurity might have entered the lattice in place of Mg(II) .

3. 4. NIR results

The NIR spectrum of the sample is shown in Fig. 2(b). In the NIR region several bands are observed in the sample. These bands are due to overtone and combination bands of water fundamentals. These bands are analysed as follows. Water has C_{2v} symmetry and gives three fundamental modes. They are ν_1 (symmetric OH stretch), ν_2 (H-O-H bending mode) and ν_3 (asymmetric OH stretch). In vapour phase, these modes occur at 3652, 1595 and 3156 cm^{-1} respectively. [31]. In solids, the occurrence of ν_1 and ν_3 are towards low wavenumber side and ν_2 towards higher wavenumber, it can be attributed to hydrogen bonding [32]. The prominent band observed at 5850 cm^{-1} with a shoulder at 5900 cm^{-1} is attributed to first overtone of fundamental stretching with a metal –OH bend [32]. The band observed at 5690 cm^{-1} is identified as overtone of ν_3 mode of H_2O molecule, where as band observed at 6870 cm^{-1} is due to $2\nu_3$ of water

molecule. The band 5480cm^{-1} is attributed to the first fundamental overtone OH stretching mode [32]. In silicate minerals, the common NIR feature appears around 7259cm^{-1} , due to ν_{OH} overtone [32]. Accordingly the very sharp band observed at 7290cm^{-1} is assigned to overtone of ν_{OH} . It indicates that water is present in the sample as trapped water in the lattice.

4. Conclusion

The optical absorption spectrum of mineral clinohumite is due to iron impurity only, which is in a distorted octahedral environment. Mössbauer results support the concept of Fe(II) in distorted octahedral structure and Fe(III) in octahedral structure. The EPR results confirm the presence of manganese and iron impurities in the mineral. Heat treatment has resulted in shifting the manganese impurities, from their current location to their lowest energy minimum configuration. NIR results confirm the presence of water fundamentals, which is also supporting the formula of the mineral.

Acknowledgements

We thank Dr. Goya, Dept. of Physics, Universidade de, de Sao Paulo, Brazil for recording the Mossbauer spectra. One of us (SLR) is thankful to UGC, New Delhi for financial assistance (project link no: 1361, March 2004). We thank the head, RSIC, IIT, Chennai for recording optical absorption spectra. The financial and infra-structure support of the Queensland University of Technology (QUT), Inorganic Materials Research Program is gratefully acknowledged. One of the authors (B. J. Reddy) is grateful to the QUT for the award of Visiting Fellowship.

References

- [1] K.K. Turekian, K.L. Wedepohl, Geol. Soc. Am. Bull. 72 (1961) 175.
- [2] J.E. Post, Proc. Natl. Acad. Sci. USA 96 (1999) 3447.
- [3] J.W. Anthony, R.A. Bideaux, K.W. Bladh, M.C. Nichols, Hand Book of Mineralogy, Vol. II, Silica, Silicates, Part 1 & Part 2, Mineral Data Publishing, Tucson, Arizona, 1995.
- [4] A.F. Wells. "Structural Inorganic Chemistry" 5th ed., Oxford University Press, Oxford University Press, Oxford (1984) 1016.
- [5] W.H. Taylor, J. West, Proc. R. Soc. London, A117 (1928) 517.
- [6] K.Robinson, G.V. Gibbs, P.H.Ribbe, H. Paul, Am. Mineral. 58 (1973) 43.
- [7] H. Strunz, E.H. Nickel, Am. Mineral. 85 (2000)1828.
- [8] N.W. Jones, P.H. Ribbe, G.V. Gibbe, Am. Mineral. 54 (1969) 391.
- [9] K.B.N.Sharma, B.J. Reddy, L.R.Murthy, S.Vedanand, B. Madhusudhana, Pak. J. Sci. Ind. Res. 33 (1990) 480.
- [10] V.V. Bukanov, A.N. Platov, M.N. Toran, E.V. Polshin, Konst. Svoistva Mineral. 11 (1977) 36.
- [11] G.H.Faye, Can. Mineral. 9 (1968) 403.
- [12] C.J. Ballhausen, Introduction to Ligand Field Theory, Mc-Graw Hill, New York, 1962.
- [13] F.A. Cotton, M.d. Megers, J. Am. Chem. Soc. 82 (1960) 5023.
- [14] O.G. Holmes, D.S. McClure, J. Chem. Phys. 26 (1957) 1686.

- [15] G.D. Jones, Phys. Rev. 155 (1967) 259.
- [16] G.H.Faye, Can. J. Earth. Sci. 5 (1968) 3.
- [17] W. Low, M. Weger, Phys. Rev. B 118 (1960) 1130.
- [18] G.M. Bancroft, R.G. Burns, A.J. Stone, Geochim. Cosmochim. Acta 32 (1968) 547.
- [19] G.M. Bancroft, R.G. Burns, Mineral. Soc. Am. Spec. Pap. 2 (1969) 137.
- [20] A. Van Abloom, E. De Grave, Phys. Chem. Miner. **23** (1996) 377.
- [21] S.G. Eeckhout, E. De Grave, C.A. Mc Cammon, R. Vochten,
Am. Mineral. 85 (2000) 943.
- [22] S.G. Eeckhout, E De Grave, C.A. Mc Cammon, R.Vochten,
Mineral. Petrol. 73 (2001) 235.
- [23] S. Lakshmi Reddy, P.S. Rao, B.J. Reddy, Phys. Lett. A 161 (1991) 74.
- [24] R.E. Vandenberghe, E. De Grave, in: Mossbauer Spectroscopy Applied
to Inorganic Chemistry, eds. G.J. Long, F. Granduan, Plenum,
New York, 1989, p 59.
- [25] Y. Tanabe, S.Sugano, J. Phys. Soc. Japn. 9 (1954) 753.
- [26] A.R. Raju, K. Muni Reddy, B.J. Reddy,
Proc. Indian natn. Sci. Acad. 49 A (1983) 662.
- [27] S.N. Reddy, R.V.S.S.N. Ravikumar, B.J. Reddy, Y.P. Reddy, P.S. Rao,
N. Jb. Miner. Mh. Jg. 2001 (6) (2001) 261.
- [28] K. Langer, R.M. Abu-Eid, Phys. Chem. Miner. 1 (1977) 273.
- [29] Geetha Ramakrishnan, M. B. V. L. N. Swamy, P. Sambasiva Rao, S. Subramanian,
Proc. Indian Acad. Sci. 103 (1991) 613.
- [30] S. Vedanand, P. Sambasiva Rao, B. J. Reddy,
Radiat. Eff. Defects Solids 127 (1993) 169.

- [31] K. Nakamoto, *Infrared Spectra of Inorganic and Coordination Compounds*, John Wiley & Sons, New York, 1970.
- [32] G. R. Hunt, J.W. Salisbury, *Mod. Geol.* 1 (1973) 283.

Table 1

Comparison of different Mossbauer parameters of iron bearing compounds

Sample	Type of ion	QS (mm/s)	IS (mm/s)	Γ (mm/s)	I (%)	Site symmetry	Ref.
Ortho pyroxene	Fe(II)	1.91	1.23			Distorted octahedron	[5]
Humite	Fe(II)	2.42	1.00			D.octahedron	[9]
	Fe(III)	1.22	0.46			D.octahedron.	
Olivine	Fe(II)	2.90	1.25			Octahedron	[24]
Almandine garnet	Fe(II)	3.55	1.40			Cubic	[26]
Plumbojarosite	Fe(III)	1.19	0.4763			D.octahedron	[23]
Clinohumite	Fe(II)	1.51	1.09	0.38	72%	D.octahedron	present work
	D site						
	Fe(III)		0.53	0.28	27%	Octahedron	
	L site						

Table 2

Band headed data with assignments for Fe(II) in clinohumite

Site I			Site II			Transitions
Wave length (nm)	Wave number (cm ⁻¹)		Wave length (nm)	Wave number (cm ⁻¹)		
	Observed	Calculated		Observed	Calculated	
1095	9130	9750	1205	8300	9050	⁵ T _{2g} → ⁵ E _g
965	10360		1020	9800		
640	15625	15637	600	16670	16528	⁵ T _{2g} → ³ T _{1g} (H)
430	23260	23253	420	23800	23719	⁵ T _{2g} → ³ T _{1g} (H)

Table 3

Comparison for different parameters of Fe(II) bearing compounds

Compound	Dq cm ⁻¹	B cm ⁻¹	C cm ⁻¹	C/B	β (%)	Reference
Triphylite	830	954	4770	5.0	90	[22]
Antigorite	990	885	3860	4.36	84	[23]
Orthoferrosilite	945	917	4040	4.40	87	[24]
	694	917	4040	4.40	87	
Clinohumite	975	900	4700	5.22	85	Present work
	905	850	4800	5.65	80	

List of Figures

Figure 1: Mossbauer spectrum of clinohumite mineral at 296 K.

Figure 2(a) Optical absorption spectrum of clinohumite at RT.

Figure 2(b) NIR spectrum of clinohumite at RT.

Figure 3: Powder EPR spectrum of the mineral clinohumite at room temperature. It indicates the presence of both Mn(II) and iron impurities. Frequency = 9.40584 GHz.

Figure 4: Expanded version of figure 3, indicating the presence of three Mn(II) impurities in the mineral clinohumite. The sixth line of manganese hyperfine resonance for the three sites is indicated by a, b and c respectively. Frequency = 9.40584 GHz.

List of Tables

Table 1 Comparison of different Mossbauer parameters of iron bearing compounds

Table 2 Band headed data with assignments for Fe(II) in clinohumite

Table 3 Comparison for different parameters of Fe(II) bearing compounds

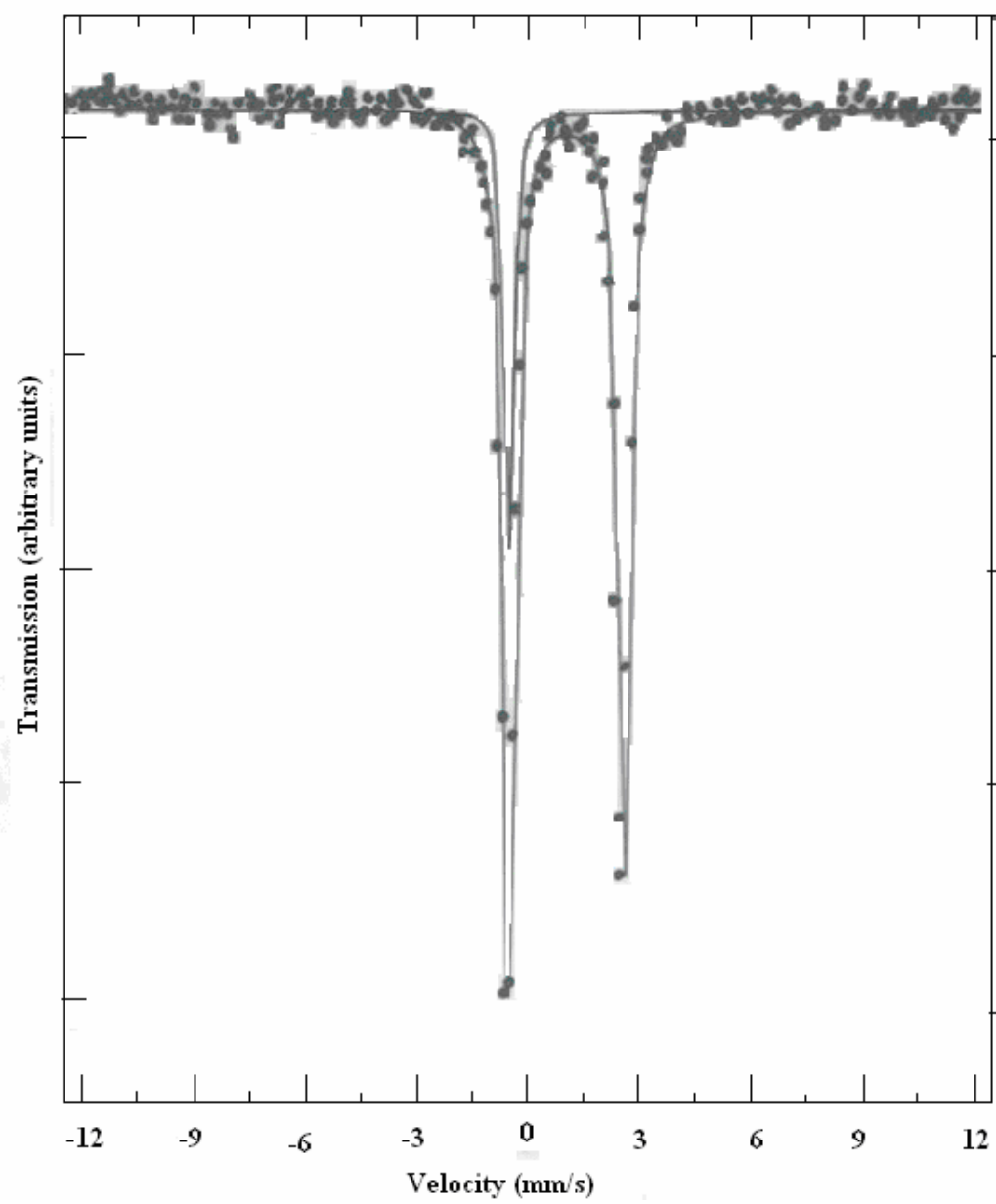


Figure 1

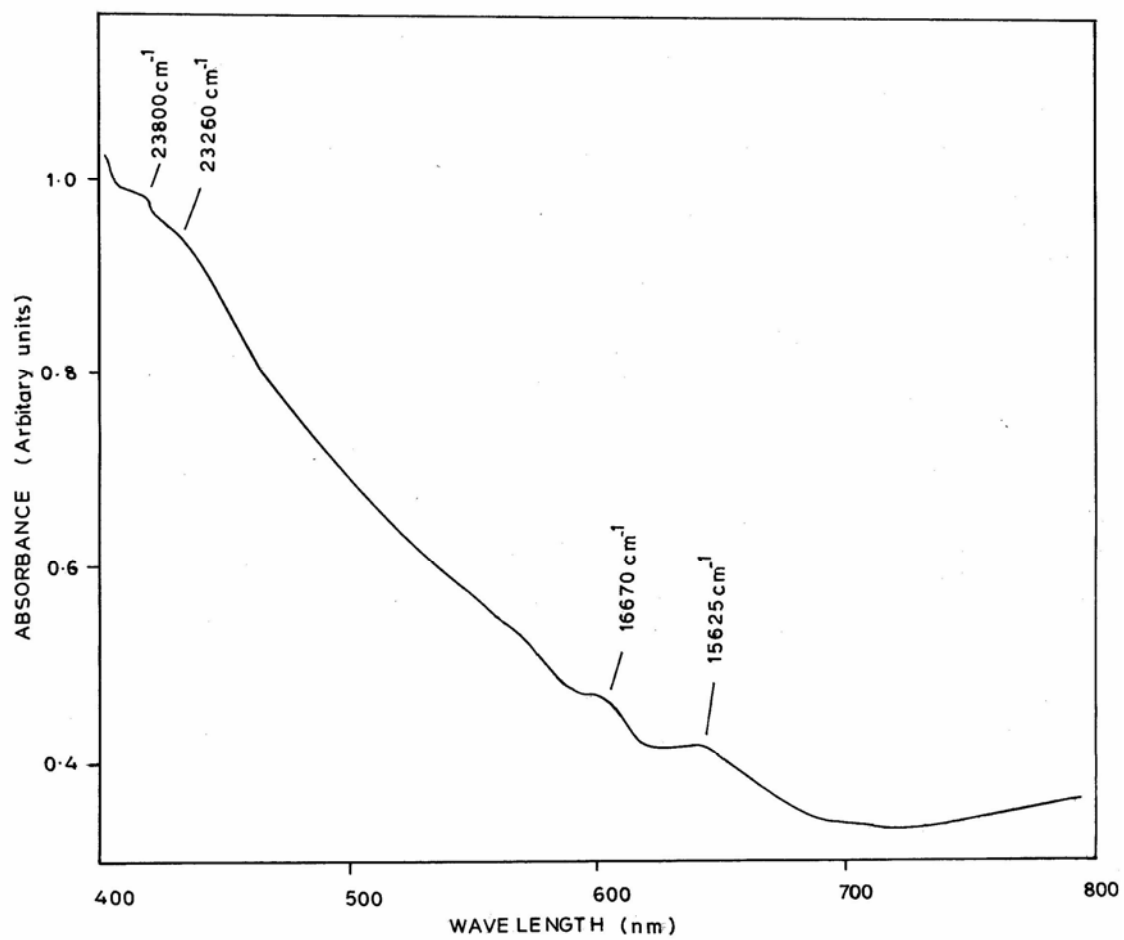


Figure 2a

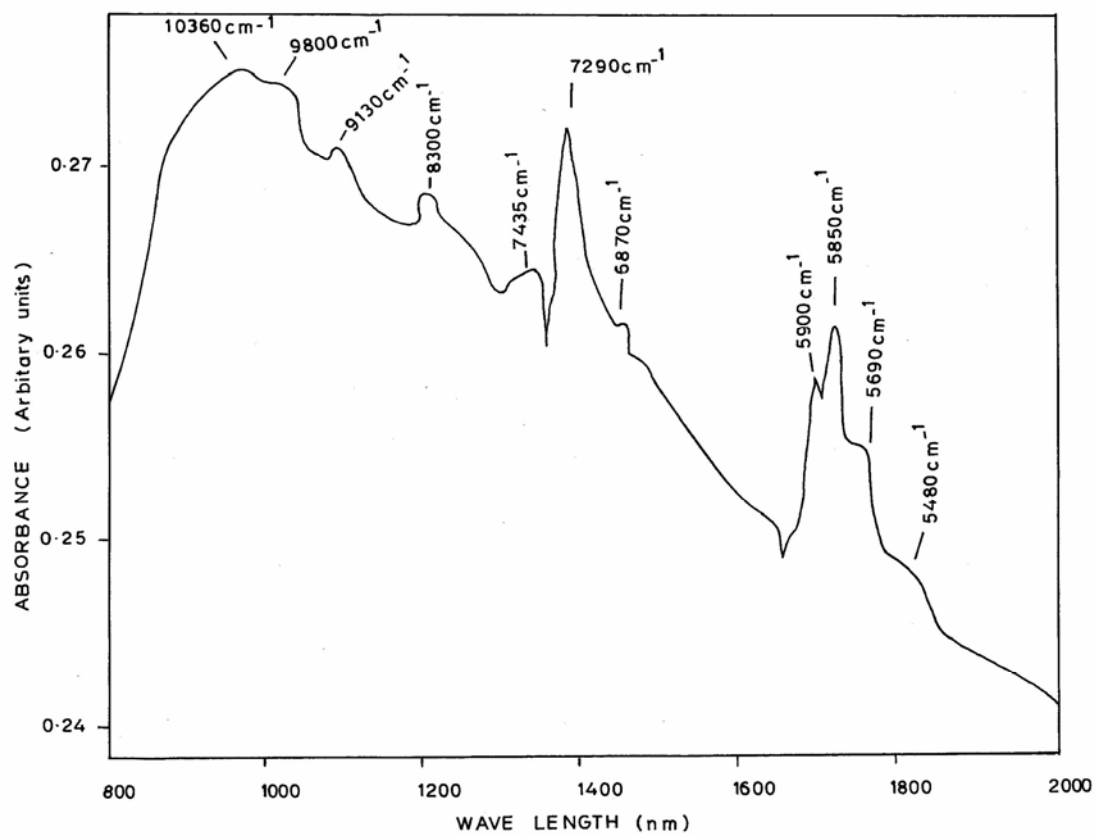


Figure 2b

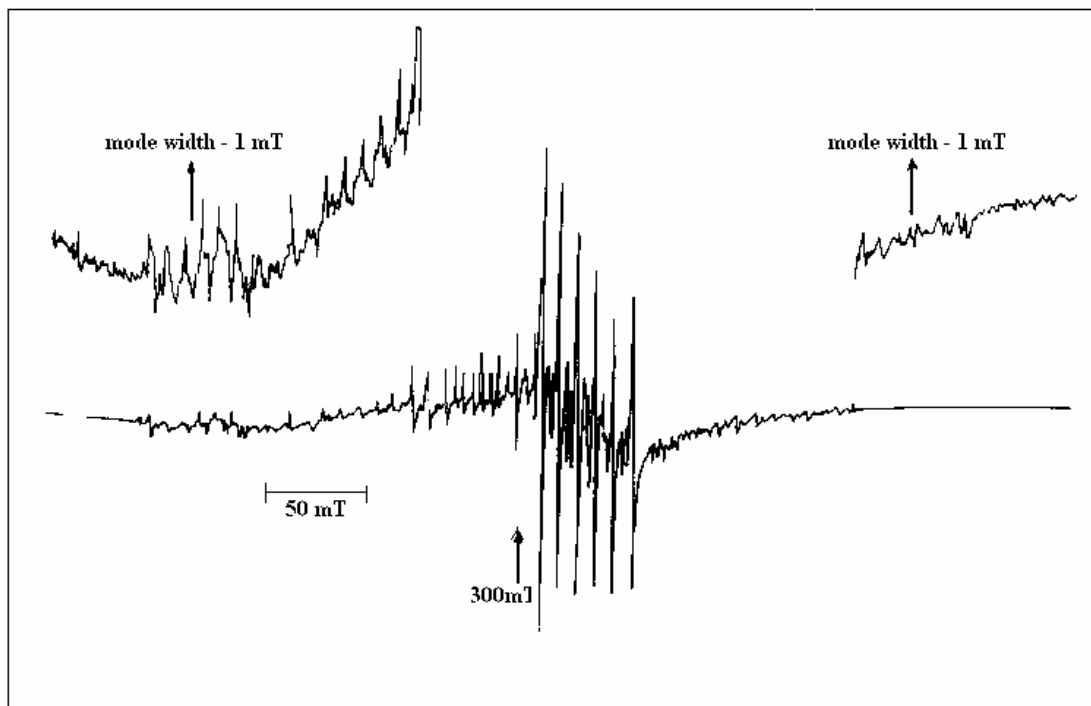


Figure 3

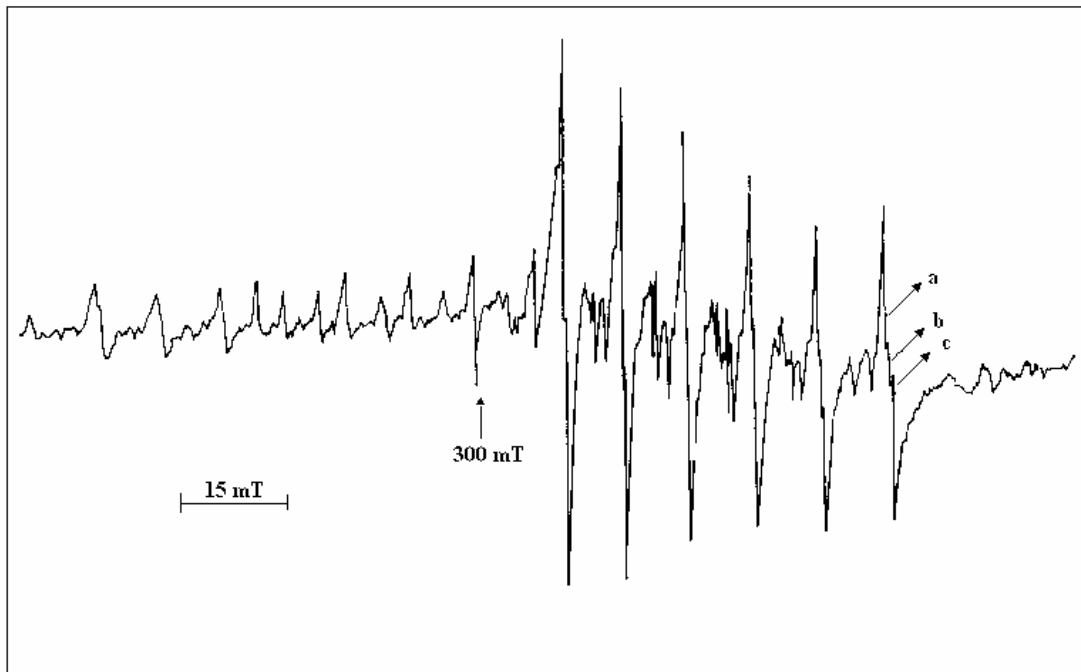


Figure 4